

Laser-driven collimated tens-GeV monoenergetic protons from mass-limited target plus preformed channel

F. L. Zheng,^{1,2} S. Z. Wu,^{1,3} H. C. Wu,¹ H. B. Cai,^{1,3} M.

Y. Yu,^{4,5} T. Tajima,⁶ X. Q. Yan,^{1,*} and X. T. He^{1,3,†}

¹*Key Laboratory of HEDP of the Ministry of Education, CAPT,
and State Key Laboratory of Nuclear Physics and Technology,
Peking University, Beijing, China, 100871*

²*Graduate School, China Academy of Engineering Physics, Beijing, China, 100088*

³*Institute of Applied Physics and Computational Mathematics, Beijing, China, 100088*

⁴*Institute of Fusion Theory and Simulation,
Zhejiang University, Hangzhou, China, 310027*

⁵*Institut für Theoretische Physik I,
Ruhr-Universität Bochum, D-44780 Bochum, Germany*

⁶*Fakultät f. Physik, LMU München, Garching, Germany, D-85748*

(Dated: February 6, 2022)

Abstract

Proton acceleration by ultra-intense laser pulse irradiating a target with cross-section smaller than the laser spot size and connected to a parabolic density channel is investigated. The target splits the laser into two parallel propagating parts, which snowplow the back-side plasma electrons along their paths, creating two adjacent parallel wakes and an intense return current in the gap between them. The radiation-pressure pre-accelerated target protons trapped in the wake fields now undergo acceleration as well as collimation by the quasistatic wake electrostatic and magnetic fields. Particle-in-cell (PIC) simulation shows that stable long-distance acceleration can be realized, and a 30 fs monoenergetic ion beam of > 10 GeV peak energy and $< 2.0^\circ$ divergence can be produced by a 9.8×10^{21} W/cm² circularly polarized laser pulse.

PACS numbers: 52.38.Kd, 41.75.Jv, 52.35.Mw, 52.59.-f

Laser-driven ion acceleration has been of much recent interest because of its broad scientific and technical applications. Protons with tens to hundreds MeV energies are useful for cancer therapy [1], high resolution imaging [2, 3], fast ignition in inertial confinement fusion [4], etc., and ions with still higher energies are relevant to high energy physics research [5], laboratory modeling of astrophysical phenomena [6], etc.

Radiation pressure acceleration (RPA) is promising for obtaining high-quality ion beams efficiently [7–9]. Existing studies have shown that GeV proton beams can be obtained by RPA using CP lasers with intensity above 10^{22} W/cm² [10, 11]. However, because of transverse instabilities and hole-boring by the laser pulse [10–12], the acceleration length is rather limited and it is difficult to enhance proton energy without still higher laser intensity. Recently, it has been shown that tens GeV proton beams [13, 14] can be generated by a moving double-layer in a possibly unlimited acceleration regime, or in a two-phase acceleration regime [15, 16] by ultra-relativistic lasers. In classical RPA and laser wakefield acceleration (LWFA), however, the accelerated ion bunch tends to diverge because of the ubiquitous space-charge field [17–19]. The resulting defocusing leads to very low ion flux. Moreover, the effective laser-plasma interaction distance is also limited by laser diffraction. As a result, ions cannot remain collimated and be stably accelerated over a long distance.

In this Letter, we propose a stable proton acceleration scheme using an ultra-intense circularly polarized (CP) laser pulse and a mass-limited target (MLT) [20] connected to a parabolic underdense plasma channel. The target splits the laser pulse into two separate but adjacent parts, which are then refractively guided by the preformed underdense plasma channel behind it. The quasistatic longitudinal accelerating and transverse collimating fields associated with the electron return current at the center of the channel can stably trap, collimate, and further accelerate the RPA target protons by LWFA over a long distance. In contrast to the existing acceleration schemes, both proton defocusing and laser diffraction do not occur. PIC simulations show that ultrashort (30 fs) monoenergetic proton beams with peak energy > 10 GeV and divergence angle $\leq 2.0^\circ$ can be obtained with a $\sim 10^{22}$ W/cm² circularly polarized (CP) laser pulse.

To demonstrate the proposed scheme we use the two-dimensional (2D) PIC code KLAP [10, 21]. The CP laser pulse is of wavelength $\lambda = 1 \mu\text{m}$ and peak intensity $I_0 = 9.8 \times 10^{21}$ W/cm² (or the normalized laser parameter $a_0 = 60$). It has a super-Gaussian radial profile with spot size $2\sigma = 40\lambda$ and a $18T$ flattop envelope, where T is the laser period. The fully

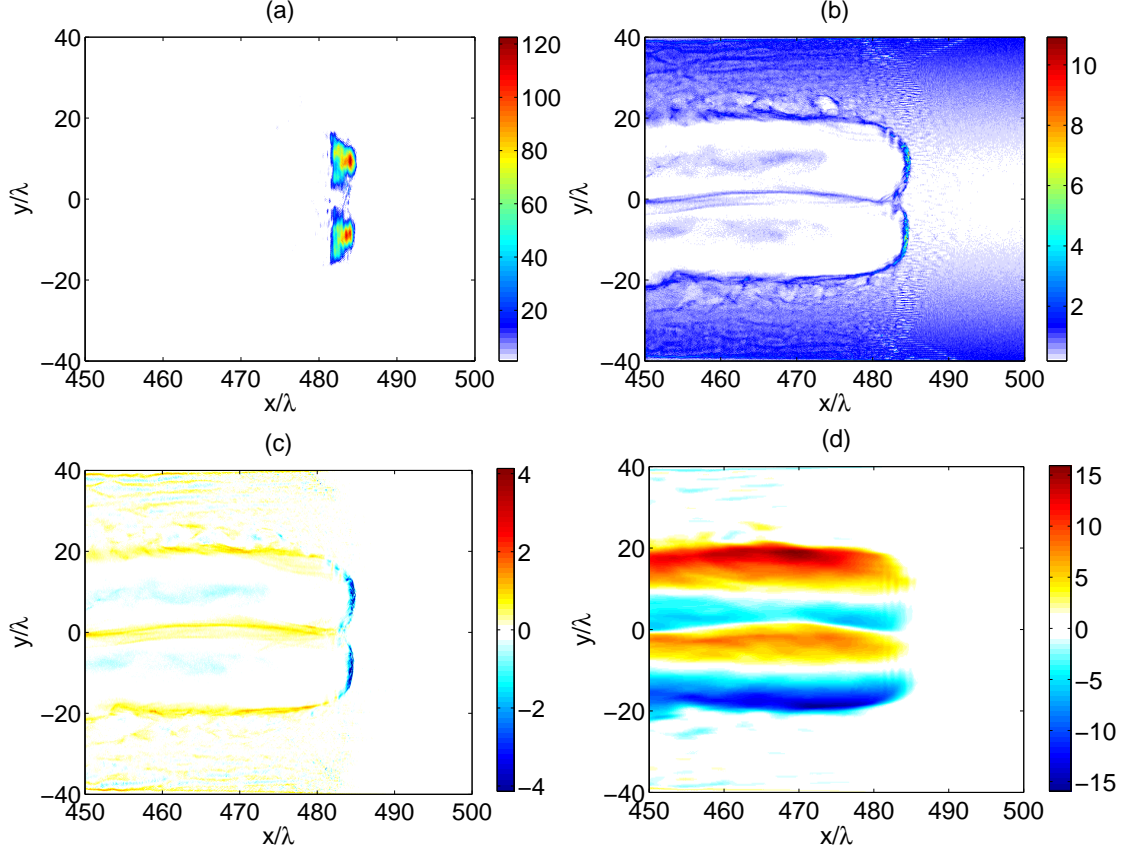


FIG. 1: (Color online) (a) Laser electric field $\sqrt{E_y^2 + E_z^2}$, normalized by \mathcal{E}_0 . (b) Electron density normalized by n_c . (c) Current density j_x normalized by $en_c c$. (d) Spatial distribution of transverse quasistatic field $E_{ys} - B_{zs}$ (in the $\pm y$ directions), at $t \sim 500T$.

ionized uniform hydrogen target of density of $N = 20n_c$, where n_c is the critical density, is located in $50\lambda \leq x \leq 50.8\lambda$, $-10\lambda \leq y \leq 10\lambda$. Behind the hydrogen target is an underdense plasma channel with a parabolic density profile $n = n_1 + \Delta n(y^2/y_0^2)$, where $n_1 = 0.15n_c$, $\Delta n = 2n_c$, $y_0 = 50\lambda$, and it is located in $50.8\lambda < x \leq 600\lambda$, $-40\lambda \leq y \leq 40\lambda$. The simulation box is of size $100\lambda \times 100\lambda$, corresponding to a moving window consisting of 3200×1000 cells, with each cell containing 800 macroparticles for the target and 6 for the underdense channel.

Figs. 1(a) and (b) show the laser intensity and electron density, respectively, at $t \sim 500T$. The transverse size h of the target is smaller than the laser spot size σ . The incoming laser pulse is split into two by the target. After passing the latter they continue to propagate forward in the preformed backside underdense plasma channel as adjacent twin pulses. The ponderomotive force of the latter expels the local plasma electrons transversely outward,

creating two adjacent wakes, or twin wakes, which trap the RPA target protons. Fig. 1(c) shows the longitudinal current density j_x at $t \sim 500T$. One can see that there is an intense electron return-current sheet between the two wakes. Since the longitudinal velocity v_x of the trapped protons is near the light speed c , the transverse field experienced by the energetic protons can be written as $\mathcal{E}\hat{e}_y = E_{ys}\hat{e}_y + c^{-1}v_x\hat{e}_xc \times B_{zs}\hat{e}_z \sim (E_{ys} - B_{zs})\hat{e}_y$, where E_{ys} and B_{zs} are the self-generated electrostatic and magnetic fields, respectively. Fig. 1(d) shows the total transverse quasistatic field $\mathcal{E} = E_{ys} - B_{zs}$ normalized by $\mathcal{E}_0 = m_e\omega c/e$, where m_e and $-e$ are the electron mass and charge, and ω and c are the laser frequency and light speed, at $t \sim 500T$. One can see that the twin wakes act as a moving potential well for confining, stabilizing, and further accelerating (now by LWFA) the RPA protons for a long distance in underdense plasma. In addition, since the target electrons also move with the twin wakes, the expelled plasma electrons are prevented from rapidly refilling the back side of the channel, so that the latter remains open for a long distance. This scenario differs significantly from that of the classical bubble/blowout acceleration regimes [22].

When the initial laser pulse is split by the target, the effective spot size σ_1 of each of the resulting twin light pulses is less than that of the original pulse. Similarly, the divergence angle $\theta_d = \sigma_1/Z_R$ is larger and the Rayleigh length $Z_R = \pi\sigma_1^2/\lambda$ smaller. Earlier results have also shown that relativistic self-focusing cannot prevent diffraction of intense light pulses [13, 14]. Thus, without the underdense plasma channel at the back of the target the laser-plasma interaction distance would be very limited.

However, this undesirable scenario is completely changed by the presence of the preformed parabolic density channel, here with the profile $n = [n_1 + \Delta n(y^2/y_0^2)]$, at the back of the target. The dispersion relation for relativistic light waves is $\omega^2 = c^2k^2 + \omega_p^2/\gamma$, where k and ω_p^2/γ are the wave number and effective background plasma frequency, respectively, and $\gamma \sim \sqrt{1+a^2}$ is the relativistic factor associated with the electron quiver motion. For an ultra-intense CP laser pulse ($a \gg 1$), the index of refraction is

$$\eta(y) \sim \left[1 - \frac{1}{a(y)n_c}(n_1 + \Delta n \left(\frac{y^2}{y_0^2} \right)) \right]^{1/2}, \quad (1)$$

so that refractive light guiding (RLG) occurs if $d_y\eta < 0$. Light diffraction can then be canceled by RLG if the maximum beam focusing angle is larger than the divergence angle θ_d , or

$$\frac{n_1}{2n_c} \left[\frac{1}{a(\sigma)} - \frac{1}{a(h/2)} \right] + \frac{\Delta n}{n_c} \left[\frac{\sigma^2}{a(\sigma)y_0^2} - \frac{(h/2)^2}{a(h/2)y_0^2} \right] \geq \left(\frac{\lambda}{\pi\sigma_1} \right)^2, \quad (2)$$

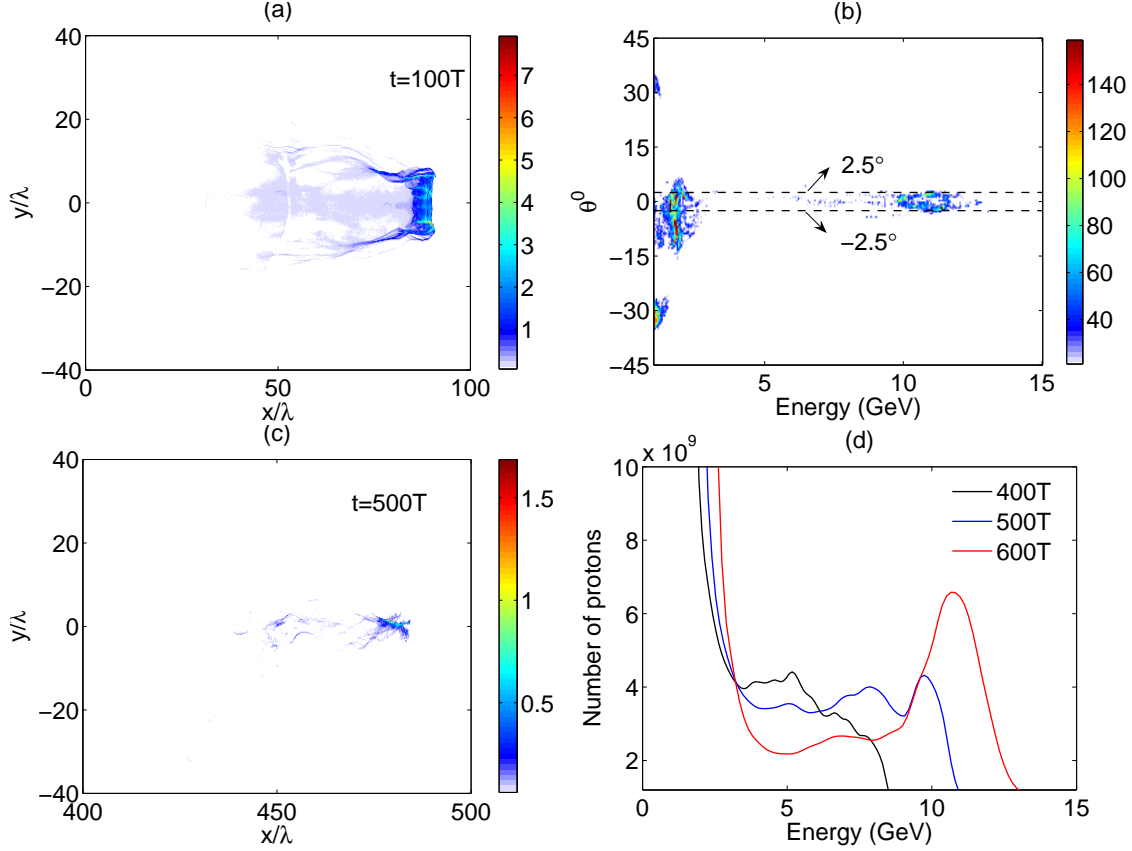


FIG. 2: (Color online) Density of the accelerated protons in units of n_c at (a) $t \sim 100T$ and (c) $t \sim 500T$. (b) Angular distribution of the protons at $t \sim 600T$. The dashed lines correspond to the divergence angle $\pm 2.5^\circ$. (d) Evolution of the proton energy spectrum.

where the three terms of the inequality represent relativistic self-focusing guiding, preformed density channel RLG, and light diffraction, respectively. We note that this relation differs considerably from that of the $a \ll 1$ case. For the parameters under consideration, the self-focusing and RLG terms in Eq. (2) have the values ~ 0.0021 and 0.013 , respectively. The latter alone is already much larger than the diffraction term, which has the value 0.0041 . One can also see that without RLG the proton bunch would diverge. Fig. 1(a) shows the profile of the light field at $t \sim 500T$. We see that RLG by the preformed parabolic density channel indeed results in long distance propagation of the twin light pulses and the corresponding twin wakes. In fact, the laser-plasma interaction distance is effectively increased to $\sim 7Z_R$. Moreover, the focusing effect of RLG also doubles the intensity of the twin pulses to $a_1 = 120$, as can be seen in Fig. 1(a).

We now consider the evolution of the pre-accelerated protons in more detail. From Figs.

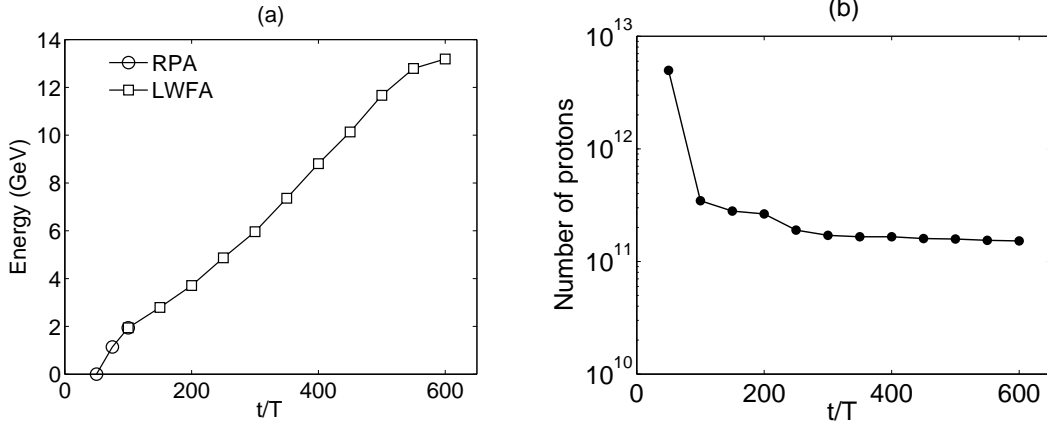


FIG. 3: (Color online) Evolution of the (a) maximum proton energy, and (b) number of protons in the axis region ($|y| \leq 3\lambda$).

2(a) and (c) one sees that the relativistic protons are confined along the original laser axis and they can propagate a long distance without divergence. Fig. 1(d) shows that the maximum quasistatic transverse (or focusing) field \mathcal{E}_{\max} induced by the charge separation and the return current at the center of the channel is about $6\mathcal{E}_0$, agreeing well with the theoretical prediction $\mathcal{E}_{\max}/\mathcal{E}_0 \sim (\pi/2)(a_1 n_1/n_c)^{1/2}$ [22]. The angular distribution of the accelerated protons at $t \sim 600T$ is given in Fig. 2(b), which shows that the average emission angle for protons with energy greater than 8 GeV is less than 2.0° . That is, the output proton beam is well collimated by the transverse quasistatic field.

Fig. 3(a) shows the evolution of the maximum proton energy. One can see the two stages of the acceleration process, namely RPA and LWFA. In the initial RPA regime, the maximum proton velocity reaches $0.945c$, or 1.93 GeV, at $t \sim 100T$. The pre-accelerated protons then undergo LWFA in the twin wakes until the light pulses are almost depleted at $t \sim 600T$. At that time, the trapped proton bunch approaches the front of the twin wakes, indicating that the dephasing length is roughly the same as the pump depletion length. We also see that the maximum proton energy increases rapidly with time and then saturates at $t \sim 600T$. Fig. 2(d) shows the evolution of energy spectrum. One can see that the latter improves with time and eventually achieves a sharp peak at about 12 GeV, which is also consistent with that of a theoretical model [15] $W_{\max} \simeq (a_1^2 n_c/n_1) m_e c^2/6$. Fig. 3(b) shows that the number of protons in the region $|y| \leq 3\lambda$ first decreases and then becomes constant at 1.5×10^{11} , indicating that the transverse spreading effect for the energetic protons is well

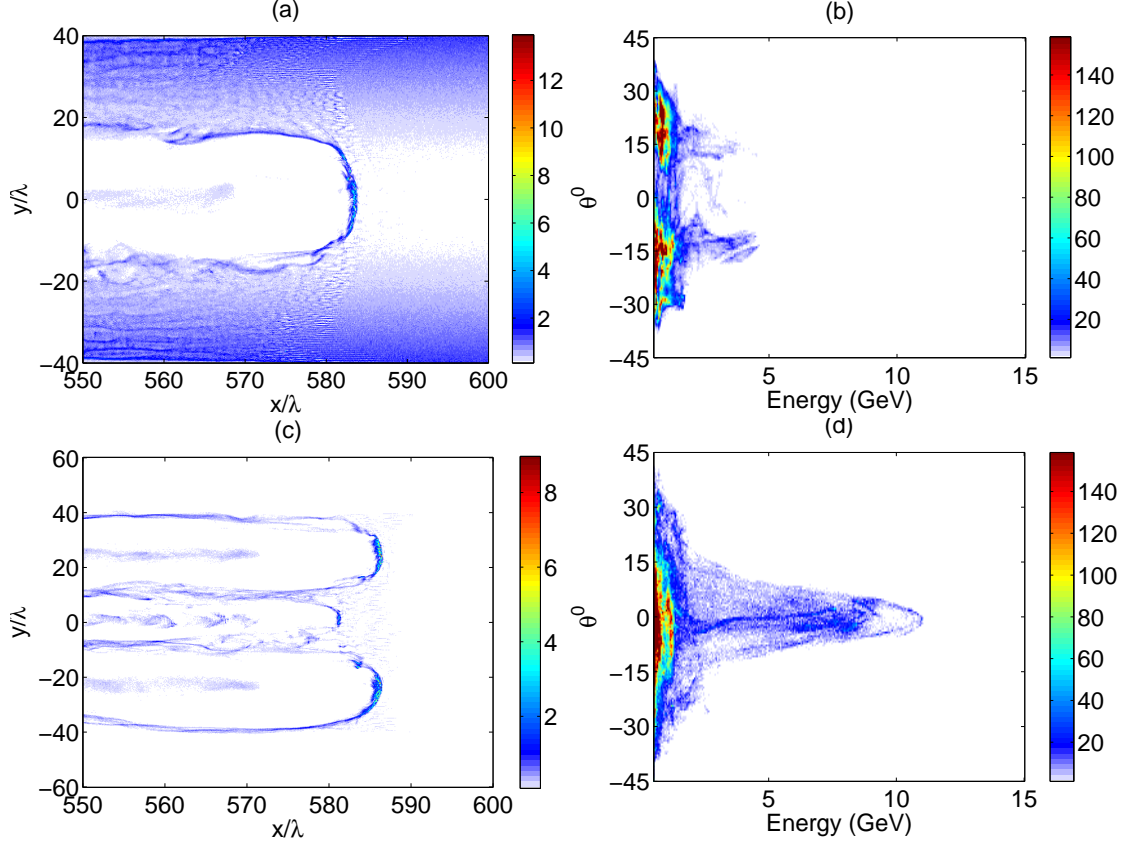


FIG. 4: (Color online) Electron charge distributions at $t \sim 600T$ for the (a) single-wake (when the condition $h \leq \sigma$ is not satisfied) and (c) twin-wakes cases. The corresponding angular distributions of the protons are shown in (b) and (d), respectively.

controlled in the backside channel. Their total energy is above 500 J and the laser conversion efficiency is about 10%. The accelerated protons are well compressed in the phase space and the quasi-monoenergetic pulse has a duration of about 30 fs. Such a short proton pulse can be used to excite a plasma wakefield that can in turn accelerate the plasma electrons [23].

A key issue in the proposed scheme is the formation of a stable proton focusing and collimating twin-wakes structure that moves at relativistic speed with the target-modulated laser light. When the transverse size of target is too large comparing to the laser spot size, the initial laser pulse can fully interact with the target. The laser is not split into two parts and no twin wakes are formed. Without the transverse confinement in the underdense region, the RPA protons would diverge. This can be seen in the simulation by setting $h = 2\sigma = 40\mu\text{m}$, with the other laser and plasma parameters the same as in the preceding simulations. Fig. 4(a) shows that instead of the stable twin wakes (see Fig. 1(b)) a single

channel is generated by the laser pulse. Due to the defocusing effect of the space-charge field, the RPA protons quickly diverge in the wake, as can be seen in Fig. 4(b) for the emission angle (almost 20°) at $t \sim 600T$. In addition, protons that deviate from the axis region do not experience LWFA. The maximum energy of the accelerated protons is about 5 GeV, which is lower than that in the stable twin-wakes case (see Fig. 2(d)). The quality of the final proton bunch is thus relatively poor in terms of energy gain as well as emission angle.

The condition (2) for guiding the laser light in the underdense plasma is also important. If the maximum focusing angle is less than the beam divergence angle, RLG of the twin pulses in the density channel cannot occur. Instead, the acceleration process becomes unstable [13, 14]. To see this, we set $\Delta n = 0$ (uniform plasma behind the target), with the other parameters unchanged. That is, the density-channel guiding effect is removed. Since the relativistic self-focusing term is less than the beam diffraction term. Fig. 4(c) shows the density distribution of electrons in this case. We see that although a twin-wakes structure is still formed at the beginning, it does not survive for a long time. Only a fraction of the RPA protons is further accelerated and for a much shorter distance than that in the preformed channel. In addition, the average divergence angle is now rather large, namely 14° , as shown in Fig. 4(d).

In conclusion, an efficient laser-driven proton acceleration scheme using a small target with a preformed parabolic underdense channel behind is proposed. The laser pulse drives RPA protons and is split by the small target into two parts, which excite behind them a twin-wakes structure in the channel. The pre-accelerated RPA target protons are efficiently collimated and further accelerated by LWFA in the wake. With this scheme, both light diffraction and proton defocusing are overcome, making long-distance acceleration possible. The conditions and characteristics of proton acceleration from the PIC simulations agree well with that from the analytical estimates. It is shown that ultrashort (30 fs) highly-collimated monoenergetic proton bunches with peak energy > 10 GeV can be produced with a 60 fs CP laser pulse of intensity 9.8×10^{21} W/cm². These bunches may be superior in fs metrology in determining the validity of the OPERA type experiments for neutrino velocity [24]. Such a short and collimated proton pulse can also be promising to excite a plasma wakefield for TeV electron acceleration.

This work is supported by the National Natural Science Foundation of China (Grant nos. 10935002, 10974022, 11025523, 11175026, 11175029), and the National Basic Research

Program of China (Grant nos. 2008CB717806, 2012CB801111).

* X.Yan@pku.edu.cn

† xthe@iapcm.ac.cn

- [1] S. V. Bulanov et al., Phys. Lett. A 299, 240 (2002).
- [2] M. Borghesi et al., Rev. Sci. Instrum. 74, 1688 (2003).
- [3] C. K. Li et al., Science 327, 1231 (2010).
- [4] M. Roth et al., Phys. Rev. Lett. 86, 436 (2001).
- [5] G. A. Mourou, T. Tajima and S. V. Bulanov, Rev. Mod. Phys. 78, 309-371 (2006).
- [6] D. H. H. Hoffmann et al., Laser Part. Beams 23, 47-53 (2005).
- [7] X. Q. Yan, et al., Phys. Rev. Lett. 100, 135003 (2008).
- [8] O. Klimo et al., Phys. Rev. ST Accel. Beams 11, 031301 (2008).
- [9] A. P. L. Robinson et al., New J. Phys. 10, 013021 (2008).
- [10] X. Q. Yan et al., Phys. Rev. Lett. 103, 135001 (2009).
- [11] B. Qiao, M. Zepf, M. Borghesi, and M. Geissler, Phys. Rev. Lett. 102, 145002 (2009).
- [12] Z. M. Zhang et al., Phys. Plasmas 17, 043110 (2010).
- [13] B. F. Shen et al., Phys. Rev. ST Accel. Beams 12, 121301 (2009).
- [14] L. L. Yu et al., New J. Phys. 12, 045021 (2010).
- [15] F. L. Zheng et al., arXiv:1101.2350v2 [physics.plasm-ph].
- [16] F. L. Zheng et al., Europhys. Lett. 95, 55005 (2011).
- [17] B. Qiao et al., Phys. Rev. Lett. 105, 155002 (2010).
- [18] S. V. Bulanov et al., Phys. Rev. Lett. 104, 135003 (2010).
- [19] X. M. Zhang et al., Phys. Plasmas 17, 123102 (2010).
- [20] T. Sokollik et al., New J. Phys 12, 113013 (2010).
- [21] Z. M. Sheng et al., Phys. Rev. Lett. 94, 095003 (2005).
- [22] T. Tajima and J. M. Dawson, Phys. Rev. Lett. 43, 267 (1979); A. Pukhov and J. Meyer-ter-Vehn, Appl. Phys. B 74, 355 (2002); W. P. Leemans et al., Nature Phys. 2, 696 (2006); W. Lu et al., Phys. Rev. Lett. 96, 165002 (2006).
- [23] A. Caldwell et al., Nature Phys. 5, 363 (2009).
- [24] G. Brumfiel, Nature News doi:10.1038/news.2011.554 .